

# 1 **Supplementary Material**

## 2 **Supplementary methods**

### 3 **Cell culture**

4 Human umbilical vein endothelial cells (HUVECs) were obtained and maintained as  
5 described before (Desch et al., 2016). Primary Human brain endothelial cells  
6 (HBMECs; ScienCell , USA) were grown in a 10 µg/ml Fibronectin (Sigma-Aldrich)  
7 coated surface in Endothelial Cell Medium (ECM) supplemented with 5% FBS  
8 (ScienCell), 1% endothelial cell growth supplements and 1% penicillin/streptomycin  
9 solution (ScienCell). The murine brain endothelial cell line (bEnd3; ATCC Genuine  
10 Cultures® CRL-2299™, USA) was grown in a 0.5% Gelatin coated surface in  
11 Dulbecco's Modified Eagle's Medium (DMEM) (Merck) supplemented with 10% FBS.  
12 The murine melanoma cell line Ret was maintained in RPMI-medium supplemented  
13 with 10% heat-inactivated fetal calf serum (FCS), 1% non-essential amino acids, 1%  
14 glutamic acid and 1% penicillin/streptomycin.

15

### 16 **Plasmatic VWF concentration**

17 Plasmatic VWF concentration was calculated by ELISA using a polyclonal rabbit anti-  
18 VWF antibody (Dako, Copenhagen, Denmark) and a polyclonal rabbit peroxidase-  
19 labeled anti-human VWF antibody (Dako, Copenhagen, Denmark). Human Plasma  
20 was used to create a standard curve with a defined content of VWF.

21

### 22 **Plasmatic ADAMTS13 activity**

23 ADAMTS13 activity was analyzed in the plasma of patients using a commercial  
24 screening assay kit following the instructions of the manufacturer (Technoclone  
25 GmbH).

26

### 27 **Isolation of platelets and erythrocytes**

28 Platelets and erythrocytes were isolated from freshly drawn citrate blood of human donors or  
29 mice according to the approval of the local ethics committee. Platelet-rich plasma (PRP) was

30 obtained by centrifugation (120 g, 15 min, RT) of citrated blood. PRP was then transferred into  
31 1:1 washing buffer (103 mM NaCl, 5 mM KCl, 3 mM NaH<sub>2</sub>PO<sub>4</sub>\* H<sub>2</sub>O, 5 mM HEPES, 5.5 mM  
32 Glucose) with a pH of 6.5 and supplemented with 1 U/ml of Apyrase (Sigma-Aldrich). After a  
33 second centrifugation step (120 g, 15 min, RT) the resulting platelet pellet was resuspended  
34 in 5% BSA supplemented washing buffer with a physiological pH of 7.4.

35 To provide a physiological haematocrit for the perfusion assays, erythrocytes from citrate blood  
36 were also isolated. The erythrocyte pellet was transferred into PBS (1:1) and centrifuged at  
37 800 g for 10 minutes. The supernatant and buffy coat was aspirated and the same procedure  
38 was repeated. The erythrocytes were washed with HEPES (1:1) and centrifuged at 800 g for  
39 10 minutes. The resulting supernatant was aspirated obtaining a pure pellet of erythrocytes.

40

#### 41 **Electric cell–substrate impedance sensing (Supplement)**

42 Transendothelial electrical resistance was measured with electric cell-substrate  
43 impedance sensing (ECIS). ECs were seeded into gelatine-coated 8-well ECIS slides  
44 (8W1E PET; Applied BioPhysics Inc., NY, USA) at a concentration of 1x10<sup>5</sup> cells/ well.  
45 Impedance at a frequency of 4,000 Hz was measured every 48 seconds (ECIS-zeta  
46 system; Applied BioPhysics Inc., NY, USA) while cells were continuously maintained  
47 in a humidified atmosphere at 37 °C and 5% CO<sub>2</sub>. The influence of resting platelet or  
48 the supernatant of platelets activated with Collagen type I (50 µg/ml) with or without  
49 preincubation with tinzaparin (100 IU/ml) and bevacizumab (0.65 mg/mL) on  
50 transendothelial electrical resistance was analyzed.

51

#### 52 **Quantitative real-time PCR (qRT-PCR)**

53 RNA from HBMECs was isolated using the RNeasy Mini Kit (Qiagen, Germany)  
54 according to the manufacturer's protocol. The cDNA was synthesized from 1 µg of total  
55 RNA per sample using the QuantiTect Reverse Transcription Kit (Qiagen, Germany).  
56 To determine the mRNA transcript level from cDNA, quantitative real-time polymerase  
57 chain reaction (RT-qPCR) was performed using the QuantiFast SYBR Green PCR Kit  
58 (Qiagen, Germany) and specific primers to VWF, PAR-1, VEGFR-1, VEGFR-2, p-  
59 selectin and β-actin for normalization.

60

61 **Supplemental Table 1.** Primers used:

<b>Targeted gene</b>	<b>Sequence</b>	
VWF	Forward	5'-TGGTGCAGGATTACTGCGGC-3'
	Reverse	5'-GCTTTGCCAGCAGCAGAAT-3'
PAR-1	Forward	5'-CCTGCTTCAGTCTGTGCGG-3'
	Reverse	5'-CTGGTCAAATATCCGGAGGCA-3'
VEGFR-1	Forward	5'-GCAAAGCCACAACCAGAAG-3'
	Reverse	5'-ACGTTTCAGATGGTGGCCAAT-3'
VEGFR-2	Forward	5'-CGTGTCTTTGTGGTGCCTG-3'
	Reverse	5'-GGTTTCCTGTGATCGTGGGT-3'
P-selectin	Forward	5'-CGTGGAATGCTTGGCTTCTG-3'
	Reverse	5'-TGAGCGGATGAACACAGTCC-3'
β-Actin	Forward	5'-AGAAAATCTGGCACCACACC-3'
	Reverse	5'-CCATCTCTTGCTCGAAGTCC-3'

62

63

64

65

66

67

68

69

70

71

72

73

74

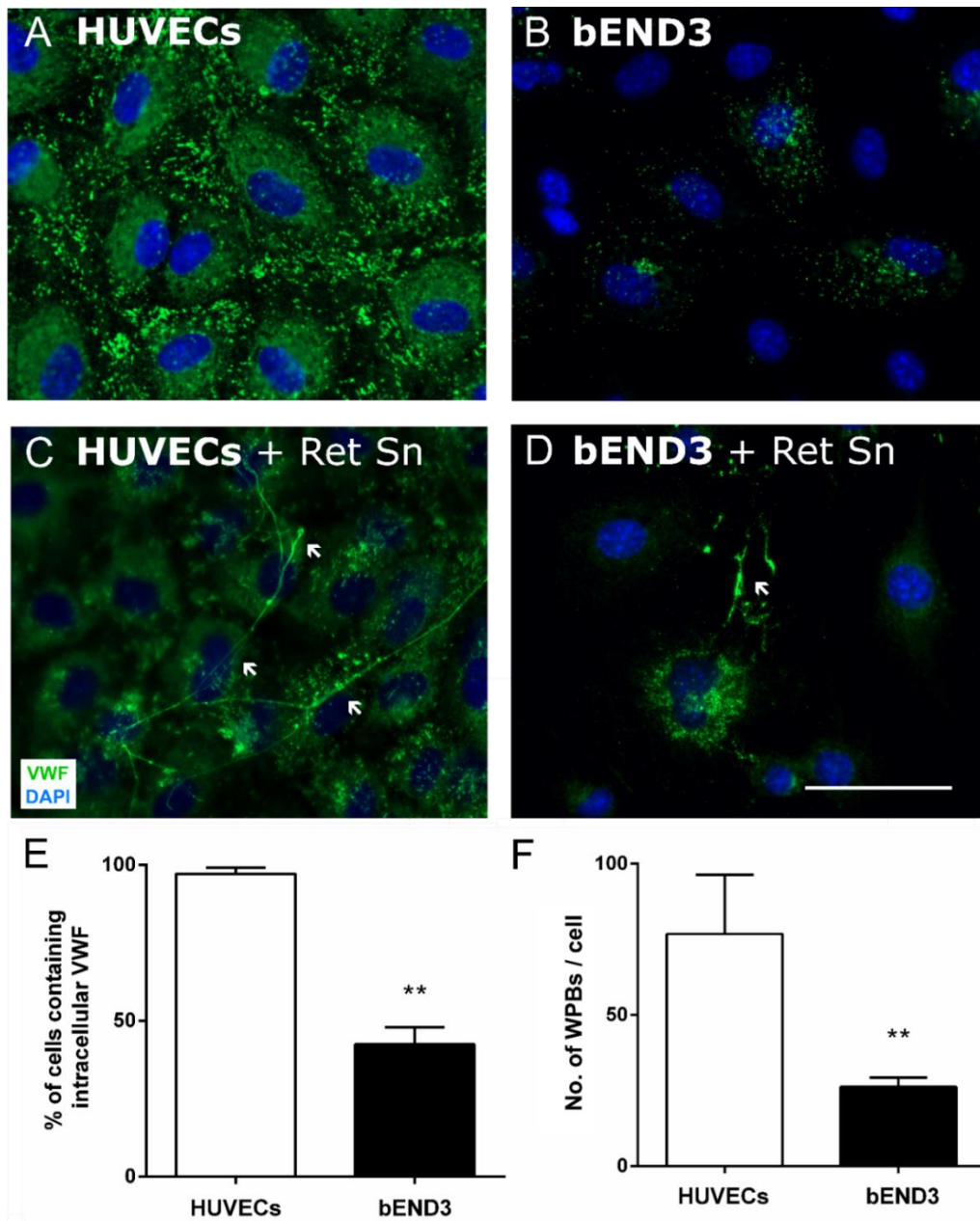
75

76

77

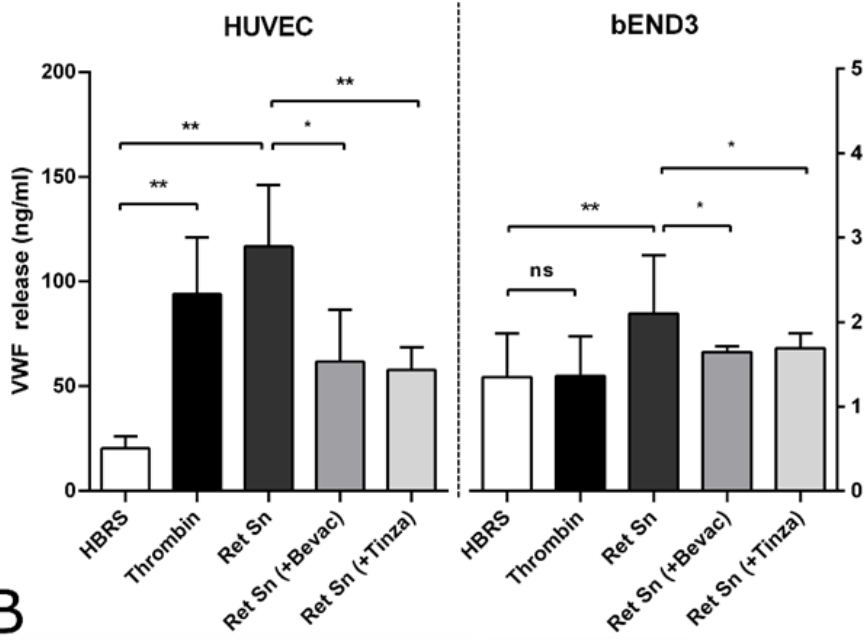
78

79

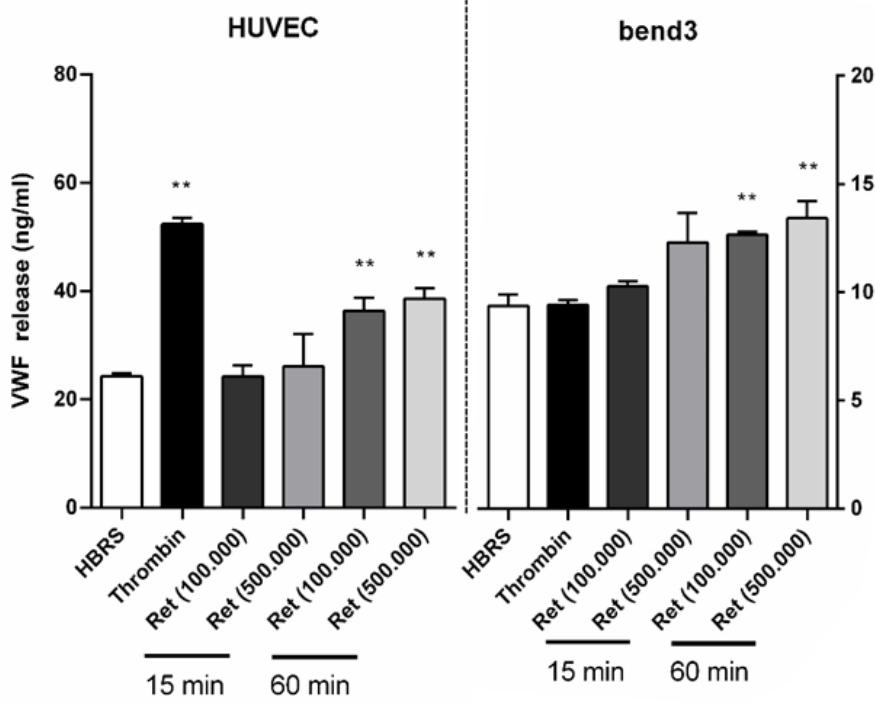


83 **Supplementary Figure 1** Immunofluorescence staining reveals a heterogeneous distribution  
 84 of Von Willebrand factor (VWF) in mouse brain endothelial cells. (A and B) Confluent quiescent  
 85 human umbilical vein endothelial cells (HUVECs) and murine brain endothelial cell line  
 86 (bEND3) were stained for VWF (green) and DAPI (blue) for nuclei. (C and D) Incubation with  
 87 the supernatant of Ret melanoma cells (Ret Sn) induced the release of VWF and the formation  
 88 of luminal VWF fibers (arrows). (E and F) The number of cells containing intracellular VWF and  
 89 the number of VWF storage intracellular granules (WPBs) per cell were quantified in HUVECs  
 90 and bEND3 (n = 50 cells/group from 3 independent experiments); \*,  $P < 0.05$ , \*\*,  $P < 0.01$   
 91 (Student *t* test). Scale bar: 50  $\mu\text{m}$ . Data are presented as mean  $\pm$  SD. Scale bar: 50  $\mu\text{m}$ .

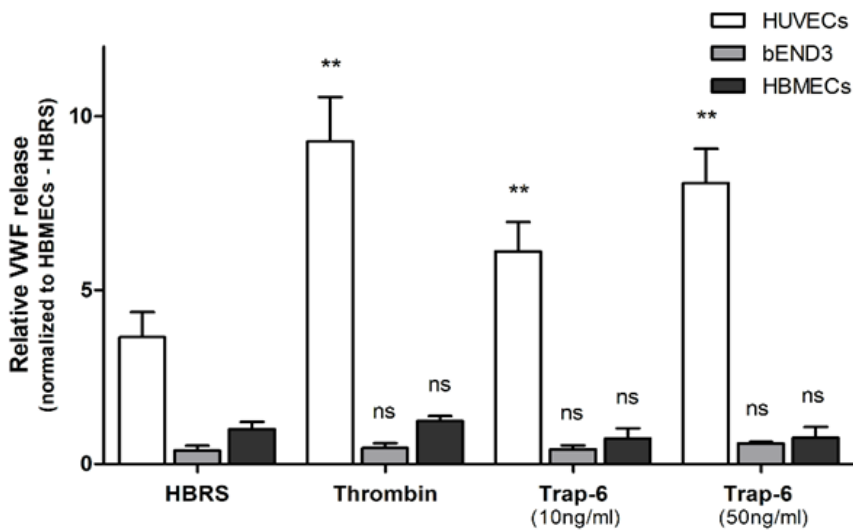
**A**



**B**



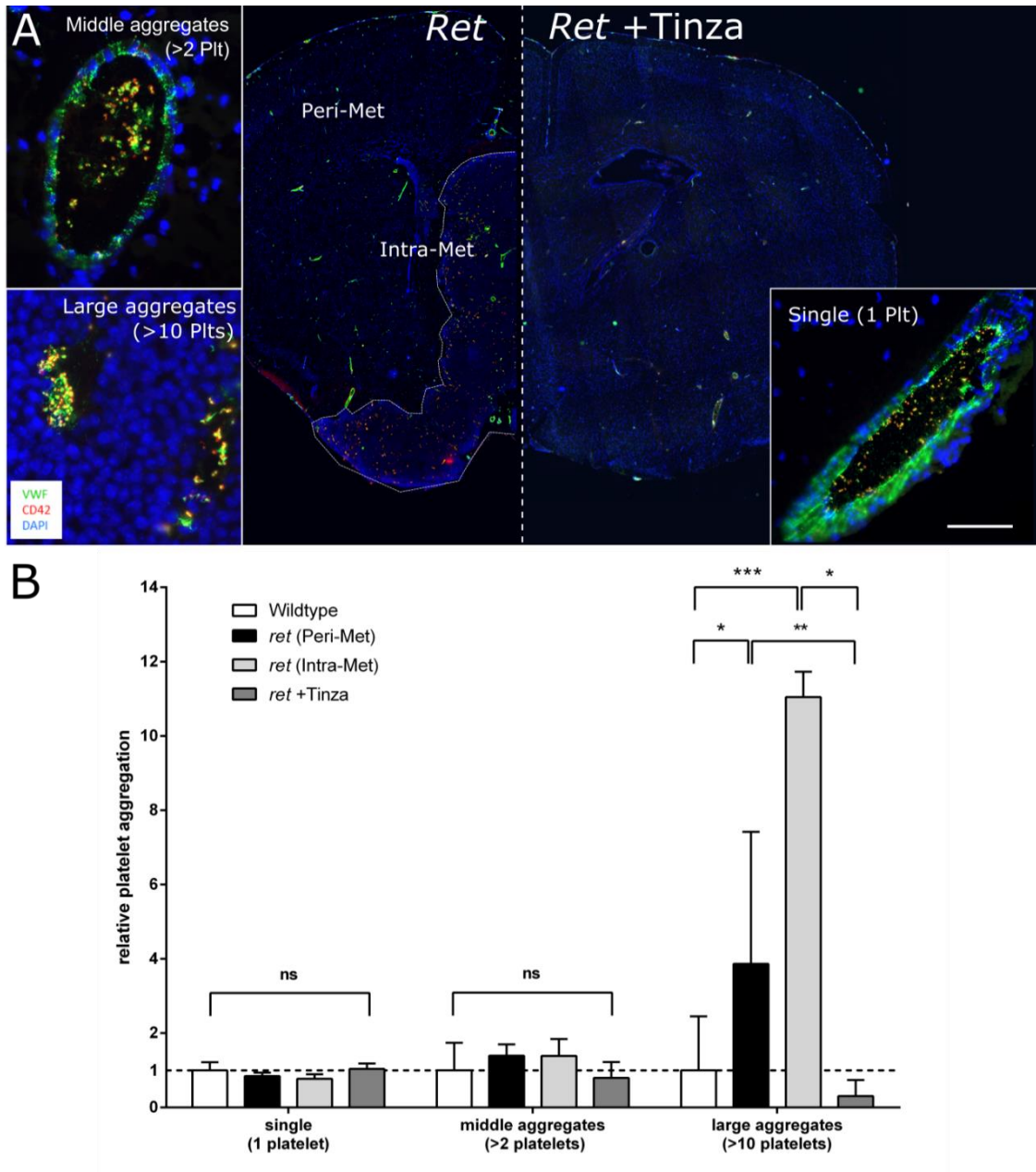
**C**



95 **Supplementary Figure 2** Activation of cerebral endothelial cells results in a minor secretion  
96 of VWF. (A) HUVECs and murine brain endothelial cells bEND3 were stimulated for 15 minutes  
97 with HEPES-buffered Ringer Solution (HBRS) as control, Thrombin (0.5 IU/ml) and Ret  
98 melanoma supernatant (Ret Sn), with or without the anti-VEGF antibody Bevacizumab (Bevac;  
99 0.65 mg/ml) or Tinzaparin (Tinza; 100 IU/ml). The concentration of VWF in cell supernatants  
100 was analyzed by ELISA (n = 6 of 2 independent experiments). (B) VWF release was measured  
101 in the supernatant of HUVECs and bEND3 after incubation with Ret cells for 15 or 60 minutes  
102 (100,00 or 500,000 Ret cells; n = 3). (C) HUVECs, bEND3 and human brain microvascular  
103 endothelial cells (HBMECs) were stimulated for 15 minutes with HBRS (Control), Thrombin  
104 (0.5 IU/ml) and different concentrations of thrombin receptor activator peptide 6 (TRAP-6) (10  
105 and 50 pg/ml). Bars show the relative differences of secreted VWF by the different cells in  
106 comparison to HBMECs treated with HBRS (n = 6-9 of 3 independent experiments); ns, not  
107 significant, \*,  $P < 0.05$ , \*\*,  $P < 0.01$  vs Control (Student *t* test). Data are presented as mean  $\pm$   
108 SD.

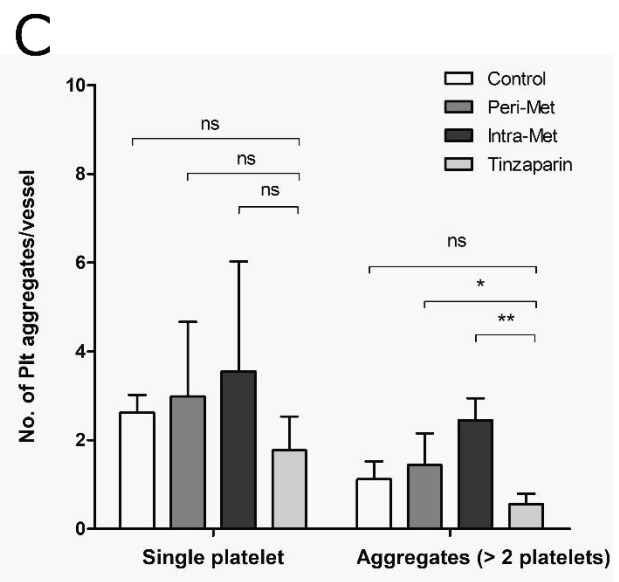
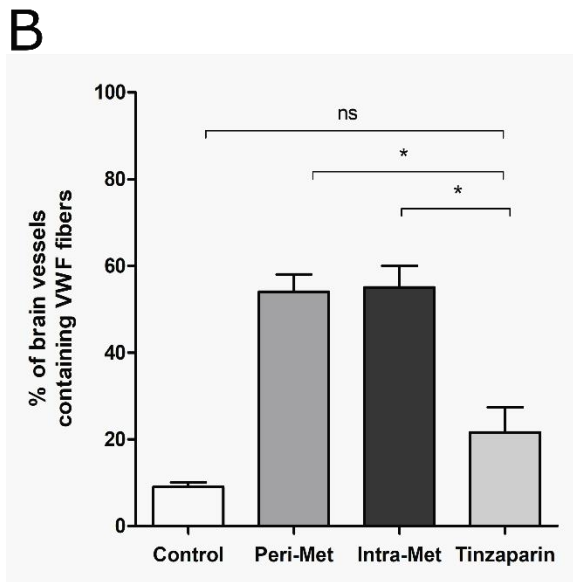
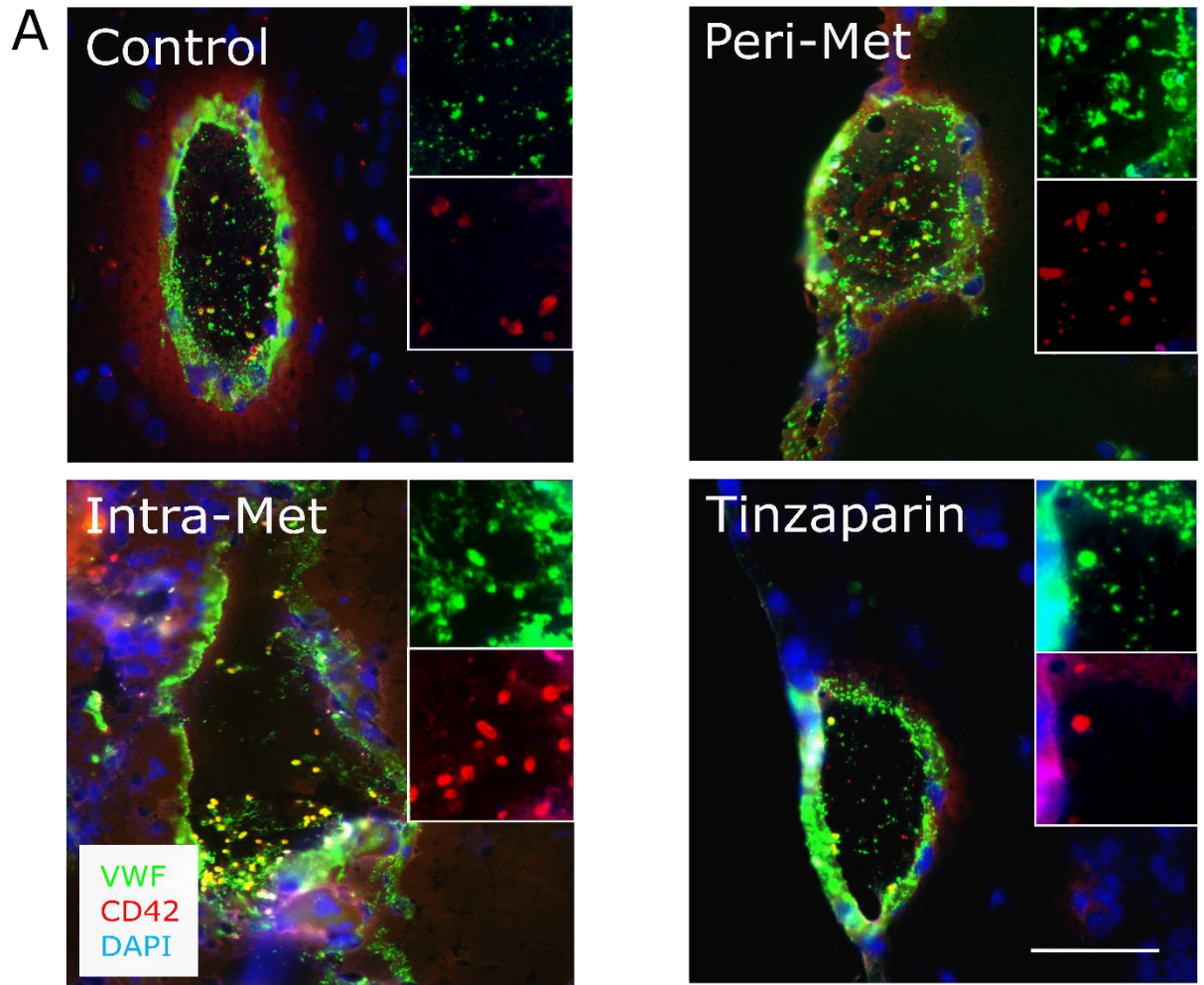
109

110  
111



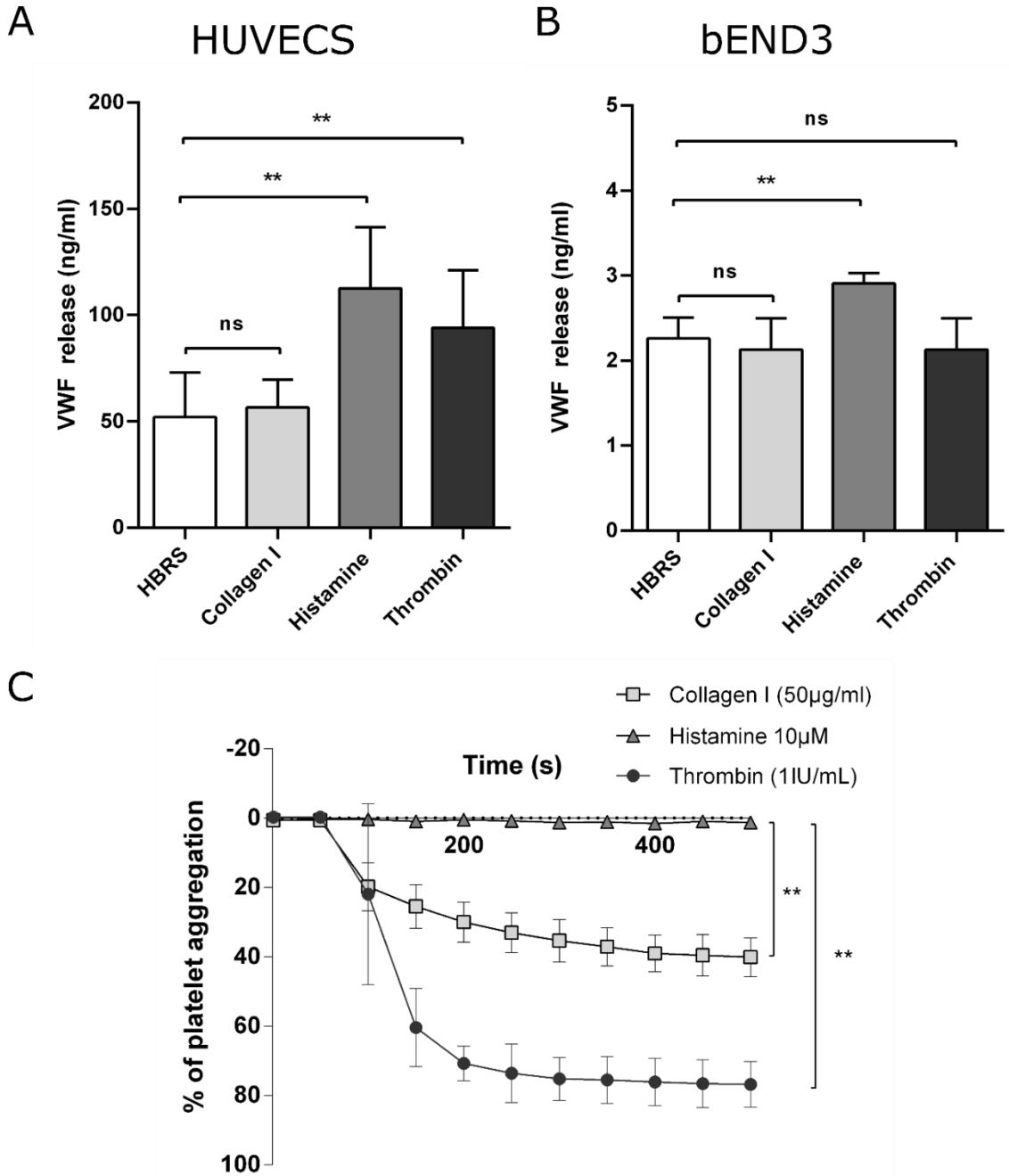
112

113 **Supplementary Figure 3** Tinzaparin inhibits the formation of large platelet aggregates *in vivo*.  
114 (A) Brain sections of wild type and *ret* mice, treated with NaCl or Tinzaparin (Tinza) (0.6 IU/g)  
115 were stained for VWF (green), CD42 (red) and nuclei (blue) with DAPI. Shown are images of  
116 two different brain sections. On the left, a brain section from a *ret* mouse treated with NaCl  
117 showing a macroscopic metastasis and on the right, a brain section from a *ret* mouse treated  
118 with Tinzaparin. The corresponding magnifications show the distribution of platelets and VWF  
119 in brain vessels from the two treated groups. (B) The number and size of intraluminal platelet  
120 aggregates was calculated in each group of mice (n = 4-6 brains per group). The corresponding  
121 quantification shows the impact of Tinzaparin on the formation of platelet aggregates, grouped  
122 by their sizes and normalized to the results in the wild type group; ns, not significant, \*,  $P <$   
123 0.05, \*\*,  $P <$  0.01 (One-way Anova). Data are presented as mean  $\pm$  SD. Scale bar: 50  $\mu$ m.



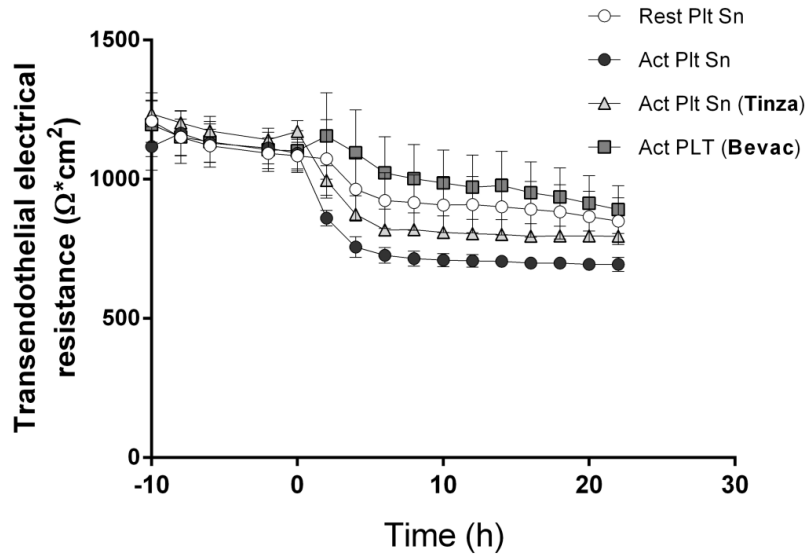


131 **Supplementary figure 4** Impact of systemic anticoagulation on intracranial hypercoagulation.  
132 Human A2058 melanoma cells were injected into the left heart ventricle of NMRI-nu/nu mice  
133 followed by anticoagulant treatment with Tinzaparin (0.6 IU/g). Brains were removed and  
134 analyzed 28 days post tumor cell injection. Brains were grouped as follows: brains from non-  
135 injected NMRI-nu/nu mice (Control), brains from injected NMRI-nu/nu mice with macroscopic  
136 metastases, which were subdivided in brain perimetastatic tissue (Peri-Met) and brain  
137 metastatic tissue (Intra-Met), and brains from injected NMRI-nu/nu mice treated with  
138 Tinzaparin (Tinzaparin). (A) Brain sections were stained for VWF (green), platelet marker  
139 CD42 (red) and DAPI (blue) for nuclei. (B) The formation of luminal VWF fibers was analyzed  
140 in each group and the corresponding quantification shows the percentage of cerebral vessels  
141 containing luminal VWF fibers in each group (n = 2-5 animals per group). (C) The area of single  
142 platelets was measured to estimate the mean number of single platelets and platelet  
143 aggregates (more than 2 platelets together) per vessel in each group (n = 2-5 brains per group);  
144 ns, not significant, \*,  $P < 0.05$ , \*\*,  $P < 0.01$  (Student *t* test). Data are presented as mean  $\pm$  SD.  
145 Scale bar: 50  $\mu$ m.  
146

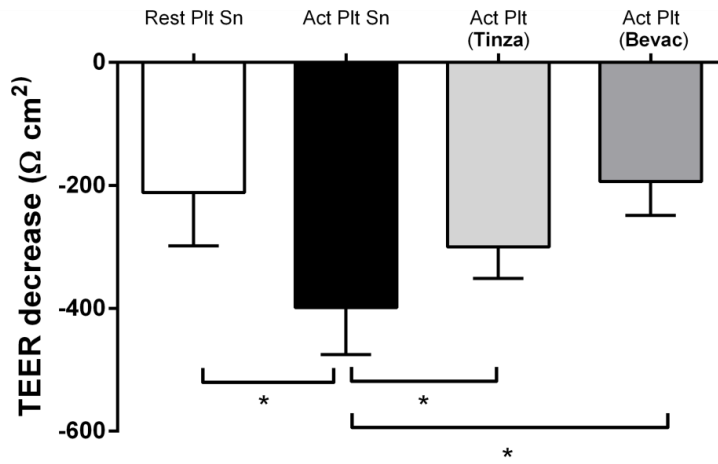


149 **Supplementary Figure 5** Activation of ECs and platelets requires different agonists. (A and  
 150 B) HUVECs and bEND3 were separately stimulated with HBRS (Control), Collagen I (50  
 151 µg/ml), Histamine (100µM) and Thrombin (0.5 IU/ml) for 15 minutes and the supernatants were  
 152 analyzed by ELISA for VWF release (n = 3 independent experiments); ns, no significant, \*\*,  
 153 P<0.01 (Student *t* test). (C) To test the impact of different agonist in platelet activation, stirred  
 154 platelets were incubated with Collagen Type I (50µg/ml), Histamine (100µM) and Thrombin  
 155 (0.5 IU/ml) and platelet aggregation was monitored for 500 seconds (s) by LTA. (n = 4  
 156 independent experiments); \*\*, P < 0.01 (F-test). Data are presented as mean ± SD.

A

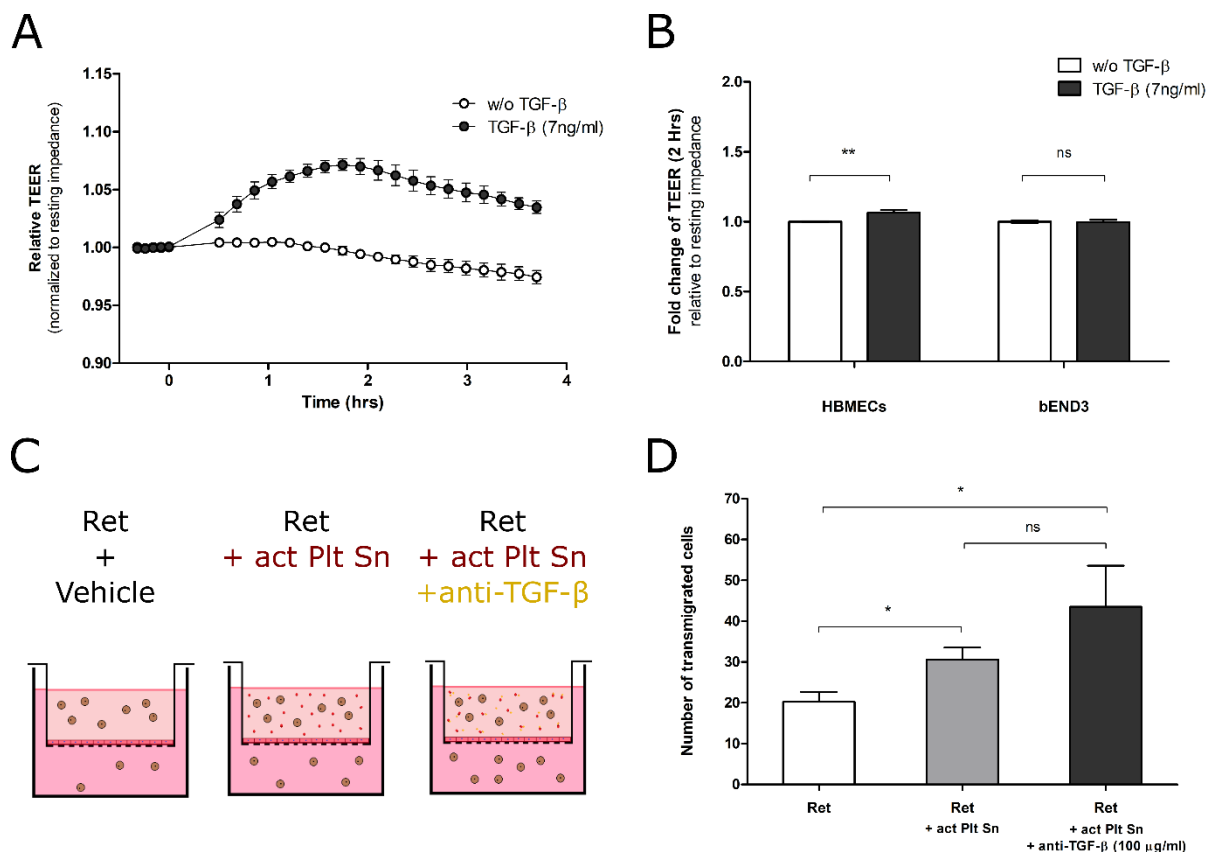


B



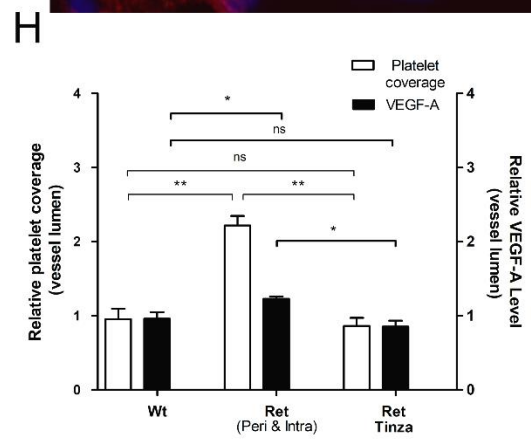
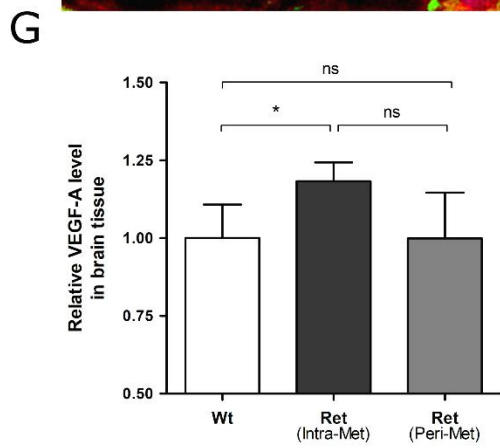
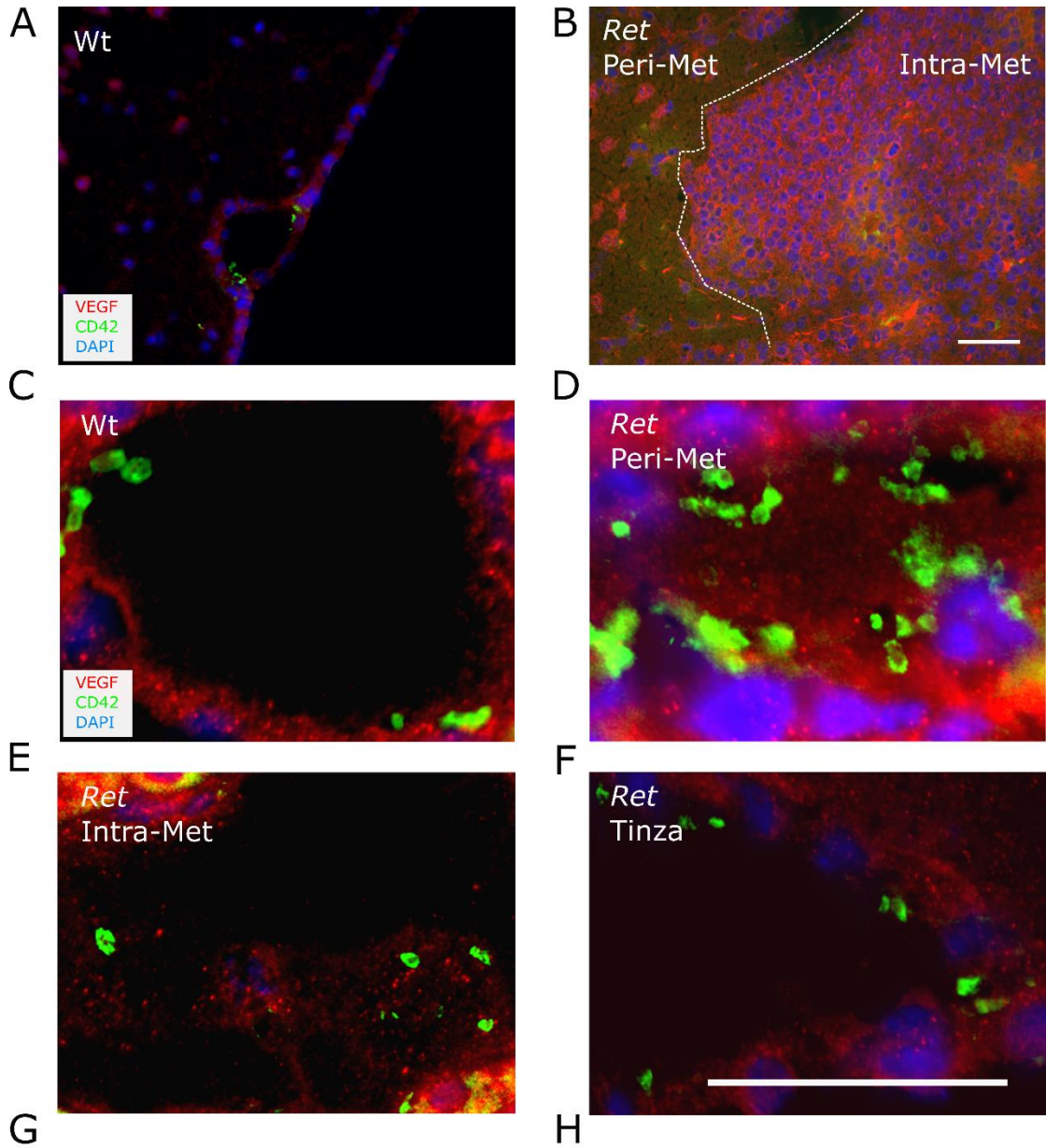
157  
158  
159  
160  
161  
162  
163  
164  
165  
166

**Supplemental Figure 6** Supernatant of activated platelets disrupts the endothelial barrier. (A) HBMEC monolayers were incubated with the supernatants of resting platelets (Rest Plt Sn) or with the supernatant of Thrombin (0.5 IU/ml)-activated platelets (Act Plt Sn), with or without a preincubation with Tinzaparin (100 IU/ml; Act Plt Sn (Tinza)) or Bevacizumab (0.65 mg/ml; Act Plt Sn (Bevac)). Transendothelial electrical resistance (TEER) was used to evaluate endothelial integrity (n = 6 of 3 independent experiment per group). (B) Bars show the absolute decrease of TEER in each group after incubation with platelet releasates. \*,  $P < 0.05$  (Student *t* test). Data are presented as mean  $\pm$  SD.



167

168 **Supplementary figure 7** Impact of transforming growth factor  $\beta$  (TGF- $\beta$ ) on tumor cell  
 169 transmigration. (A) HBMEC monolayers were incubated in presence of TGF- $\beta$  (7 ng/ml). TEER  
 170 was measured for 5 hours (hrs) after addition of TGF-  $\beta$ . Results were normalized to  
 171 impedance values measured prior to TGF- $\beta$  addition (n = 4 of 2 independent experiments). (B)  
 172 Bars show the changes in TEER in HBMECs and bEND3, when the differences were at the  
 173 maximum, 2 hours after the addition of TGF- $\beta$  (n = 4 of 2 independent experiment per group);  
 174 ns, not-significant. C, schematic diagram of the tumor cell transendothelial migration assay:  
 175 Ret melanoma cells were coincubated with HBMEC monolayers for 8 hours, alone or  
 176 supplemented with the supernatant of activated platelet (act Plt Sn). An anti-TGF- $\beta$  antibody  
 177 (100  $\mu$ g/ml) was added to test the impact of platelet-derived TGF- $\beta$  on tumor cell  
 178 transmigration. Then, upper chambers were removed and transmigrated tumor cells were  
 179 counted after 24 hours. (D) The corresponding quantification shows the number of  
 180 transmigrated Ret cells in each condition (n= 4-5 independent experiments per condition). \*,  
 181  $P < 0.05$ , \*\*,  $P < 0.01$  (Student *t* test). Data are presented as mean  $\pm$  SD.  
 182



183

184

185

186

187 **Supplementary Figure 8** Immunofluorescence staining reveals a heterogeneous distribution  
188 of VEGF-A in brain tissue during metastasis. Brain sections of wild type (Wt) and *ret* mice were  
189 stained for CD42 (green), VEGF-A (red) and DAPI (blue) for nuclei. Representative images  
190 show the differences in VEGF-A fluorescence intensity between Wt brain tissue (A) and  
191 metastatic *ret* brain (Peri- and Intra-Met tissue). (G) The quantification shows the relative fold  
192 change in the fluorescence intensity of VEGF-A in the distinct tissues normalized to the levels  
193 observed in Wt mice (n = 2-5 animals per group). (C-F) The distribution of VEGF-A was also  
194 analyzed in the lumen of brain vessels of each group and in *ret* mice treated with Tinzaparin  
195 (Tinza), the corresponding magnifications show the differences of luminal VEGF-A among the  
196 different groups. (H) Bars show the relative platelet coverage (white) and the relative fold  
197 change of luminal VEGF-A fluorescence intensity (black) in brain tissue from *ret* mice (Peri-  
198 and Intra-Met) and brain tissue from *ret* mice treated with Tinzaparin, shown results were  
199 normalized to values observed in Wt brains (n = 2-5 animals per group); ns, not significant, \*,  
200  $P < 0.05$ , \*\*,  $P < 0.01$ , (Student *t* test). Data are presented as mean  $\pm$  SD. Scale bars: 50  $\mu$ m.

201  
202

203 **Videos**

204 **Video 1**

205 The impact of platelet-derived VWF on thrombus formation was analyzed in real time by using  
206 microfluidic devices. A confluent monolayer of the murine bEND3 cells (blue) was perfused  
207 with Wt mouse platelets (red). In a first step, endothelial-derived VWF secretion was induced  
208 by histamine (100  $\mu$ M). In a second step, platelet activation and subsequent aggregation was  
209 induced by addition collagen type I (50  $\mu$ g/ml). For the visualization of VWF strings anti-VWF-  
210 FITC (green) antibody (1:100) was added (n = 4 experiments). Scale bars 50  $\mu$ m.

211

212 **Video 2**

213 The impact of platelet-derived VWF on thrombus formation was analyzed in real time by using  
214 microfluidic devices. A confluent monolayer of the murine bEND3 cells (blue) was perfused  
215 with VWF -/- mouse platelets (red). In a first step, endothelial-derived VWF secretion was  
216 induced by histamine (100  $\mu$ M). In a second step, platelet activation and subsequent  
217 aggregation was induced by addition collagen type I (50  $\mu$ g/ml). For the visualization of VWF  
218 strings anti-VWF-FITC (green) antibody (1:100) was added (n = 6 experiments). Scale bars 50  
219  $\mu$ m.

220

221